

## Verification of Lattice Spring Model for Modelling Composite Material

Wei Chian Low<sup>1</sup>, Khai Ching Ng<sup>1,\*</sup>, Hoon Kiat Ng<sup>1</sup>

<sup>1</sup> Department of Mechanical, Materials and Manufacturing Engineering, The University of Nottingham Malaysia Campus, Jalan Broga, 43500, Semenyih, Selangor Darul Ehsan, Malaysia

### ABSTRACT

The use of lattice spring model (LSM) in modelling composite material is verified using static and dynamic loading test cases. The LSM results are compared against those from finite element method (FEM) implemented in ANSYS. Simple cubic (SC) lattice structure is employed in the LSM to model 3D solid body deformation. The material symmetry used to model composite material is orthotropic. In the current preliminary study, good agreement is found between the LSM and FEM results.

#### Keywords:

lattice spring model; particle method;  
Finite Element Method

Received: 22 July 2022

Revised: 20 Sept. 2022

Accepted: 21 Sept. 2022

Published: 23 Oct. 2022

### 1. Introduction

The superior stiffness-to-weight ratio of composite materials has made it a favourable choice across many engineering applications such as ship building [1] and aerospace [2]. Composite materials could in general be divided into three groups, namely the fiber-reinforced composite, particulate composite and laminated composite. Numerical modelling of the first two types of composites could be achieved by considering the direction-dependent material strength i.e., disregarding the small-scale heterogeneous feature of the material and treat it as anisotropic homogeneous. This approach however could not be applied to laminate composite due to the presence of clear material interface and thus explicit representation of each material ply is necessary in numerical modelling of laminate composite.

In the context of numerical method for solid mechanics, continuum-based approach such as finite element method (FEM) is a well-established framework. On the other hand, mesh-less and discrete-based approach such as lattice spring model (LSM) has been very popular in solid fracture modelling [3]. In this work, we intend to validate the LSM called volume compensated particle method (VCPM) extended to model composite body [4] against FEM through test cases involving static load and dynamic load. Specifically, orthotropic material symmetry that is transversely isotropic is considered in the deformable solid body for both cases. In the literature, the extended LSM [4] had been used to model cross laminate but the dynamic deformation response of an orthotropic solid body was not investigated. Good agreement was found between the static deformation result from FEM and LSM.

\* Corresponding author.

E-mail address: [khaiching.ng@nottingham.edu.my](mailto:khaiching.ng@nottingham.edu.my)

The error convergence plot for the static loading case shows first order convergence which is similar with previous published study for the method [5]. Moreover, in dynamic loading test case, the deformation path result from LSM matches with FEM result. This shows that the extended LSM for modelling orthotropic material symmetry is accurate and has good potential in application involving composite materials.

## 2. Methodology

LSM is a particle method in which solid particles are connected to neighbouring particles through spring bonds. In current work, simple cubic (SC) lattice structure is employed to model 3D composite body. The schematic representation of SC lattice structure is shown in figure 1. In SC lattice structure, each particle has 18 neighbours (six first-nearest neighbours and twelve second-nearest neighbours).

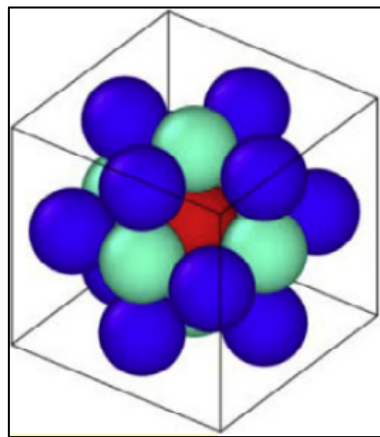


Fig. 1. Simple cubic lattice structure [4]

The spring constants for each of the 18 neighbours could be obtained by comparing the material stiffness matrices. Accordingly, the spring constant values are different, subject to the type of material symmetry and strength in each direction. Under orthotropic material symmetry, relationship between spring parameters in different directions [4] could be shown in equation 1,

$$\begin{aligned}
 k_1 &= k_2; T_1 = T_2 \\
 k_3 &= k_4; T_3 = T_4 \\
 k_5 &= k_6; T_5 = T_6 \\
 k_7 &= k_8 = k_9 = k_{10}; T_7 = T_8 = T_9 = T_{10} \\
 k_{11} &= k_{12} = k_{13} = k_{14}; T_{11} = T_{12} = T_{13} = T_{14} \\
 k_{15} &= k_{16} = k_{17} = k_{18}; T_{15} = T_{16} = T_{17} = T_{18}
 \end{aligned} \tag{1}$$

where  $k$  is the local potential and  $T$  is the non-local multibody potential. From equation 1, there are nine independent spring constants that need to be determined from the material constants. The relationship between the nine independent model parameters and stiffness matrix elements [4] could be shown in equation 2.

$$\begin{bmatrix} k_1 \\ k_3 \\ k_5 \\ k_7 \\ k_{11} = 4R \\ k_{15} \\ T_1 \\ T_3 \\ T_5 \end{bmatrix} = \begin{bmatrix} 1 & 0 & 0 & -1 & 0 & 0 & -1 & -1 & 1 \\ 0 & 1 & 0 & 0 & -1 & 0 & 1 & -1 & -1 \\ 0 & 0 & 1 & 0 & 0 & 0 & -1 & -1 & 1 \\ 0 & 0 & 0 & 0 & 0 & 1 & 0 & 0 & 0 \\ 0 & 0 & 0 & 0 & 1 & 0 & 0 & 0 & 0 \\ 0 & 0 & 0 & 1 & 0 & 0 & 0 & 0 & 0 \\ 0 & 0 & 0 & -13/54 & 5/54 & 5/54 & -5/54 & -5/54 & 13/54 \\ 0 & 0 & 0 & 5/54 & -13/54 & 5/54 & 13/54 & -5/54 & -5/54 \\ 0 & 0 & 0 & 5/54 & 5/54 & -13/54 & -5/54 & 13/54 & -5/54 \end{bmatrix} \begin{bmatrix} C_{11} \\ C_{22} \\ C_{33} \\ C_{44} \\ C_{55} \\ C_{66} \\ C_{13} \\ C_{12} \\ C_{23} \end{bmatrix} \quad (2)$$

The force between the particle of interest, I and particle J could be computed from the derivative of potential of unit cell with respect to half the change in length of spring between the particles as shown in equation 3,

$$F_{IJ} = -\frac{\partial U_{cell}}{\partial \delta l_{IJ}} \hat{u}_{IJ} = -k_I \delta l_{IJ} - \frac{T}{2} \left( \sum_{J=1}^{18} \delta l_{IJ} + \sum_{M=1}^{18} \delta l_{JM} \right) \quad (3)$$

where  $\hat{u}_{IJ} = r_I - r_J / \|r_I - r_J\|$  is the displacement vector between particle I and J,  $\delta l_{IJ}$  is the half of change in length between spring connecting particle I and J.

### 3. Results and Discussion

The first validation test case involves hanging beam under the effect of gravity. The geometry of the beam is shown in figure 2. For orthotropic material that is transversely isotropic, five independent elastic constants are required. The material constants used for this test case are  $E_x = 15MPa$ ,  $E_y = E_z = 0.8MPa$ ,  $\nu_{xy} = 0.32$ ,  $\nu_{yz} = 0.29$ ,  $G_{xy} = 0.46MPa$  and the density applied is  $1500 \text{ kg/m}^3$ . The top surface of the beam is fixed and the principal material direction is along the length of beam. The simulation for VCPM case was run until  $t=0.5 \text{ s}$  and with a damping coefficient of 50.

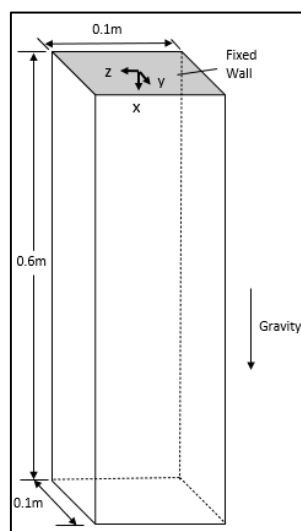


**Fig. 2.** Hanging beam under effect of gravity

Comparison between the steady state result from VCPM and FEM is done by measuring the deformation along the midline of the beam due to gravity as shown in figure 3. From the plot, as the particle spacing of VCPM is refined, convergence to the grid-independent result of FEM is observed. The spatial convergence test is given in figure 4 where the error is measured against FEM result at the free end of beam.

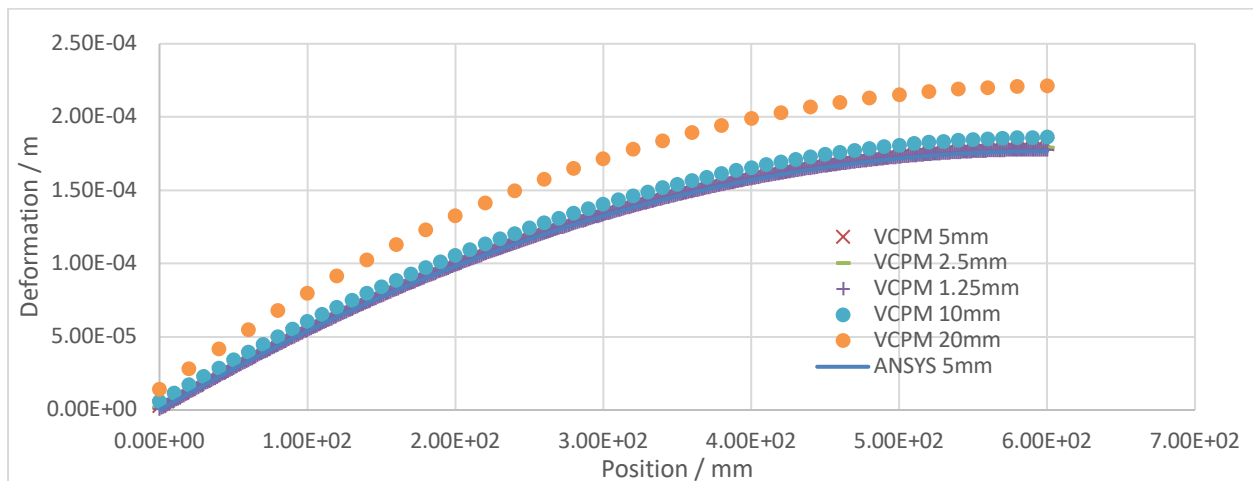


**Fig. 3.** Plot of midline deformation against position along the beam

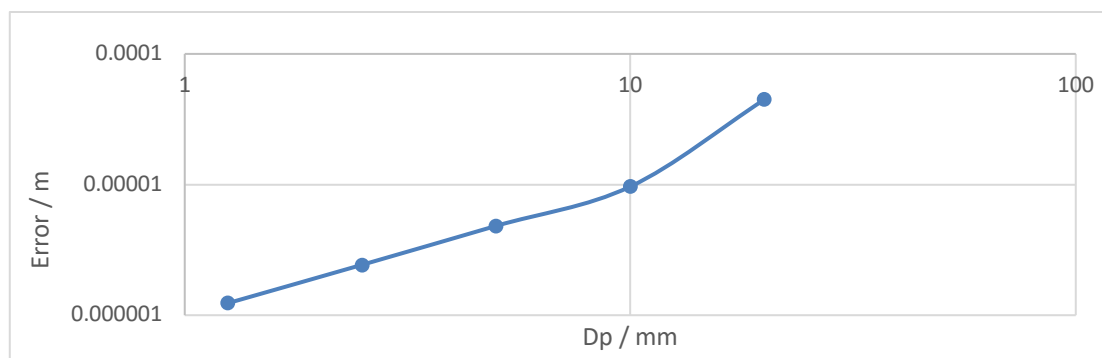


**Fig. 4.** Spatial convergence error plot at free end

Next, second test case is dynamic loading on cantilever beam where the geometry is shown in figure 5. The magnitude of dynamic load applied on the edge of the beam shown in figure 5 is zero at  $t=0$  s and increases linearly to 0.1 N at  $t=0.5$  s. The material properties for this test case are the same as the first test case and the principal material direction is along the length of beam (x-direction in figure 5). Result of deformation of top vertex at free end of beam is compared against time-step-size-independent and grid-independent result from FEM. From figure 6, the deformation at the top free end vertex of the beam agrees well with the result from FEM. It is also noteworthy that the time evolution of deformation path in this case is different from another similar case that used isotropic material [6]. For isotropic material, the deformation path evolution is smooth whereas as shown in figure 6, the deformation evolution for orthotropic material shows presence of “stair-like” path.

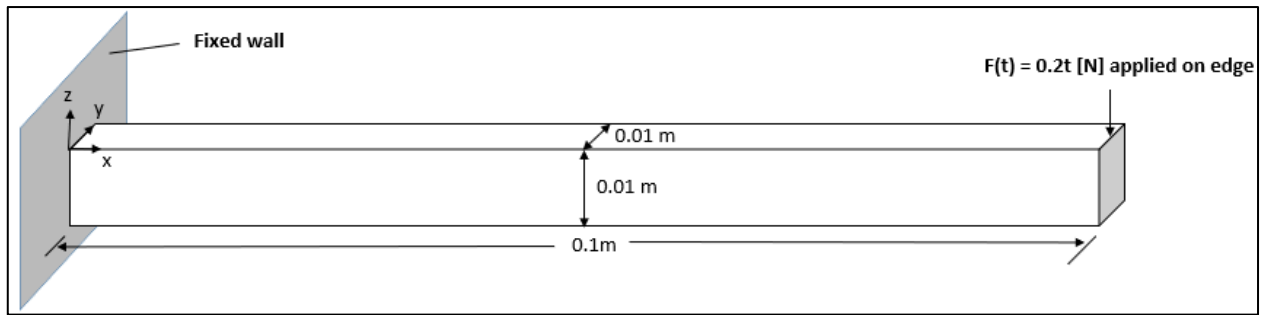


**Fig. 5.** Dynamic loading on cantilever beam

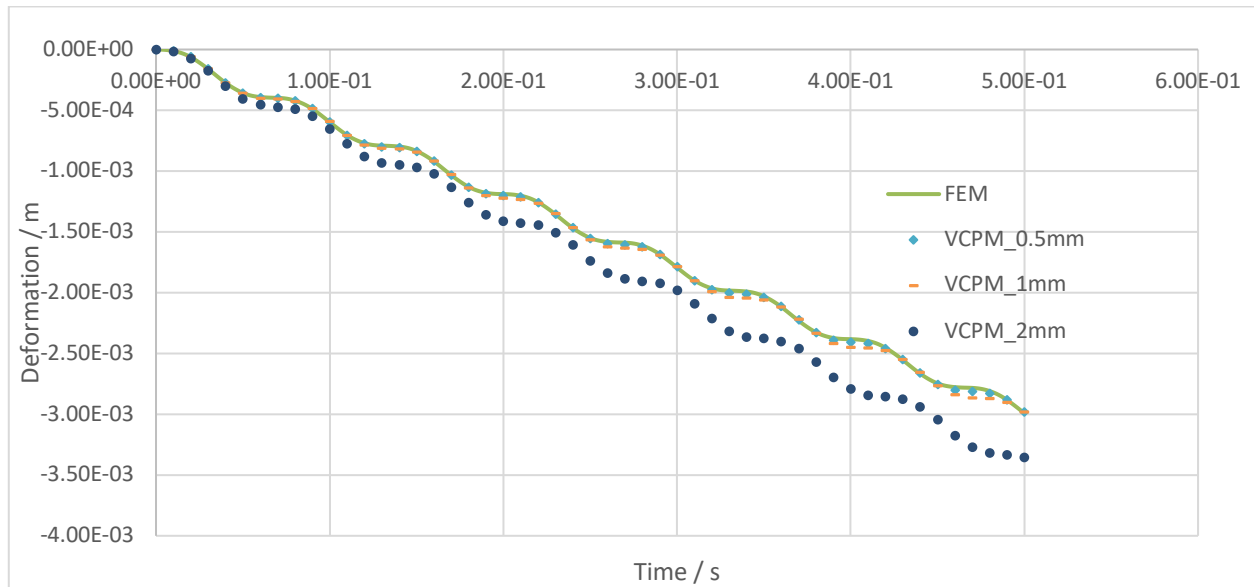


**Fig. 6.** Plot of deformation of free end vertex of beam against time

#### 4. Conclusion

Modelling of composite material using VCPM has been validated against FEM through static and dynamic loading test cases. The result from LSM agrees well with FEM's result on both test cases. This modelling approach that considers only the direction-dependent material strength property of composite material is applicable to fibrous and particulate composite but not laminate. Future investigation should focus on the dynamic response of laminate composite modelled using LSM and its suitability in practical engineering applications.

#### References

- [1] Mouritz, A. P<sup>†</sup>, Evan Gellert, Peter Burchill, and Karen Challis. "Review of advanced composite structures for naval ships and submarines." *Composite structures* 53, no. 1 (2001): 21-42. [https://doi.org/10.1016/S0263-8223\(00\)00175-6](https://doi.org/10.1016/S0263-8223(00)00175-6)
- [2] Giurgiutiu, Victor. "Fundamentals of Aerospace Composite Materials.[In] Structural Health Monitoring of Aerospace Composites." (2015). <https://doi.org/10.1016/B978-0-85709-523-7.00016-5>
- [3] Chen, Hailong, Enqiang Lin, Yang Jiao, and Yongming Liu. "A generalized 2D non-local lattice spring model for fracture simulation." *Computational Mechanics* 54, no. 6 (2014): 1541-1558. <https://doi.org/10.1007/s00466-014-1075-4>

- [4] Chen, Hailong, and Yongming Liu. "Deformation and failure analyses of cross-ply laminates using a nonlocal discrete model." *Composite Structures* 152 (2016): 1007-1013.  
<https://doi.org/10.1016/j.compstruct.2016.06.054>
- [5] Ng, K. C., A. Alexiadis, Hailong Chen, and T. W. H. Sheu. "A coupled smoothed particle hydrodynamics-volume compensated particle method (SPH-VCPM) for fluid structure interaction (FSI) modelling." *Ocean Engineering* 218 (2020): 107923. <https://doi.org/10.1016/j.oceaneng.2020.107923>
- [6] Zhan, Ling, Chong Peng, Bingyin Zhang, and Wei Wu. "A stabilized TL–WC SPH approach with GPU acceleration for three-dimensional fluid–structure interaction." *Journal of Fluids and Structures* 86 (2019): 329-353.  
<https://doi.org/10.1016/j.jfluidstructs.2019.02.002>